Human Molecular Genetics, 2006, Vol. 15, No. 6 ***921–931***
doi:10.1093/hmg/ddl009
Advance Access published on January 31, 2006

Impaired helix 12 dynamics due to proline 892 substitutions in the androgen receptor are associated with complete androgen insensitivity

Youssef A. Elhaji[1,2,*], Ileana Stoica[4], Sheldon Dennis[4], Enrico O. Purisima[4] and Mark A. Trifiro[1,2,3]

[1]Lady Davis Institute for Medical Research, Sir Mortimer B. Davis Jewish General Hospital, [2]Department of Human Genetics, [3]Department of Medicine and [4]Biotechnology Research Institute, McGill University, National Research Council of Canada, Montreal, Que., Canada

Received November 20, 2005; Revised and Accepted January 27, 2006

Structural studies of the ligand-binding domain (LBD) of several steroid receptors have revealed that the dynamic properties of the C-terminal helix 12 (H12) are the major determinant of the activation mode of these receptors. H12 exhibits high mobility and different conformations in the absence of ligand. Upon ligand binding, H12 is stabilized in a precise position to seal the ligand-binding pocket and finalize the assembly of the activation function (AF-2) domain. In this study, we investigated the role of the conserved proline 892 of the androgen receptor (AR) in directing the dynamic location and orientation of the AR-H12. We used a combined approach including kinetic and biochemical assays with molecular dynamic simulations to analyze two substitutions (P892A and P892L) identified in individuals with complete androgen insensitivity syndrome. Our analyses revealed distinct mechanisms by which these substitutions impair H12 function resulting in severely defective receptors. The AR-P892A receptor exhibited reduced ligand binding and trans-activational potential because of an increased flexibility in H12. The AR-P892L substitution renders the receptor inactive due to a distorted, unstructured and misplaced H12. To confirm the mutants' inability to stabilize H12 in an active position, we have developed a novel *in vivo* assay to evaluate the accessibility of the H12-docking site on the AR-LBD surface. An extrinsic AR-H12 peptide was able to interact with wild-type and mutant LBDs in the absence of ligand. Ligand-induced proper positioning of the intrinsic H12 of wild-type AR prevented these interactions, whereas the misplacement of the mutants' H12 did not. Proline at this position may be critical for H12 dynamics not only in the AR, but also in other nuclear receptors where this proline is conserved.

INTRODUCTION

Normal development of the male phenotype and reproductive system requires pre- and postnatal androgen actions. These actions are mediated by the androgen receptor (AR), a ligand-activated transcription factor that belongs to the nuclear receptor superfamily (NR3C4) (1). The AR is encoded by an X-linked gene. Thus, in XY individuals, any loss-of-function mutation in the single AR copy results in androgen insensitivity (2). Androgen insensitivity syndrome (AIS) is a spectrum ranging from female phenotype in complete AIS (CAIS) to male phenotype with infertility and/or gynecomastia in mild AIS (MAIS), with a wide range of partial insensitivity (PAIS) in-between (2). As a nuclear receptor, the AR has the conserved modular structure consisting of an N-terminal domain (NTD) that contains a constitutive activation function (AF-1), a central DNA-binding domain (DBD) and a C-terminal ligand-binding domain (LBD) that contains a hormone-dependent activation function (AF-2) (Fig. 1A).

A vast majority of the reported AR mutations are amino acid substitutions within the LBD (3). Different substitutions at the same amino acid may result in variable impact on the

*To whom correspondence should be addressed at: Lady Davis Institute for Medical Research, Department of Human Genetics, McGill University, 3755 Cote-Ste-Catherine Road, Montreal, Que., Canada H3T 1E2. Fax: +1 5143407502; Email: youssef.elhaji@mail.mcgill.ca

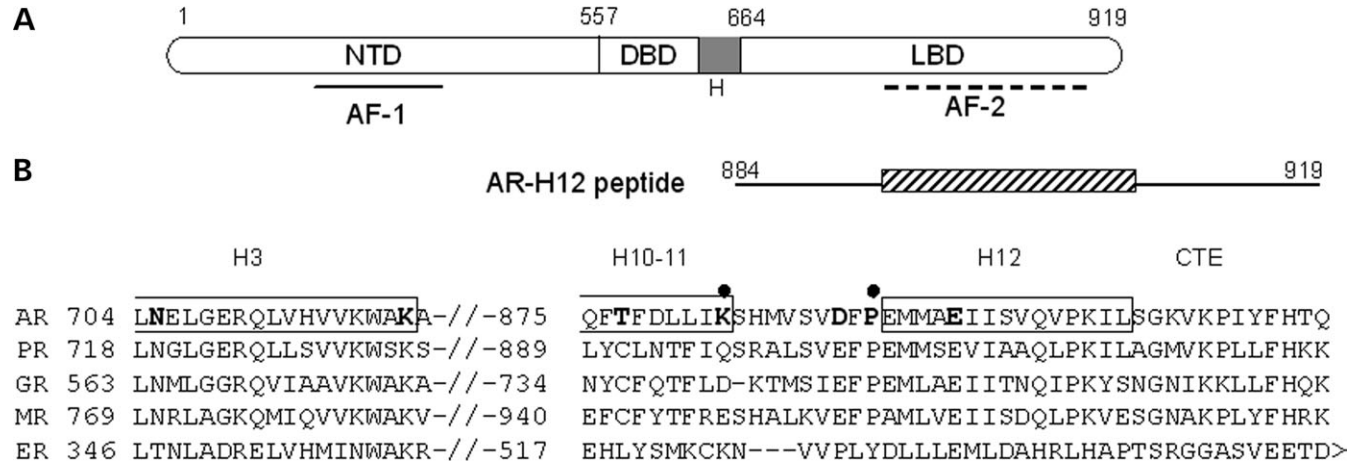

Figure 1. Schematic representation of the AR structure/function organization and sequence alignment with other steroid receptors. (**A**) The AR modular structure: an NTD, a central DBD, a hinge region (H) and a C-terminal LBD. The AR has two main activation functions: a constitutive (AF-1) in the NTD and a hormone-dependent (AF-2) in the LBD. (**B**) Sequence alignment of the C-termini of H3 and the C-terminal portions (starting at the end of H10–11) of the LBDs of steroid receptors. The AR-H12 peptide used for the H12 interaction assay is also shown. Mutation sites, P892 and K883, are indicated by filled circles and the AR-conserved residues discussed in the text are in bold.

activity of the receptor leading to different degrees of AIS (4,5). Some amino acids appear to be absolutely required for the AR function as any substitution results in a completely inactive receptor leading to CAIS phenotype (3) (database of reported AR mutations is available at http://www.androgendb.mcgill.ca/).

X-ray crystallographic studies of the agonist- and antagonist-bound AR-LBD (6–9) and other NR-LBDs (10 and references therein) revealed that all NR-LBDs share a common three-dimensional structure encompassing 12 α-helices. These α-helices undergo similar conformational changes in response to ligand binding resulting in the assembly of the AF-2 domain. This domain is formed by residues from helices 3, 4, 5 and 12 and constitutes a conserved hydrophobic cleft flanked by opposing-charge clusters (8,10,11). The AR AF-2 domain provides overlapping binding sites for conserved LXXLL motifs in NR co-activators and, with higher affinity, for FXXLF and WXXLF motifs located in the AR-NTD (8,11). AR AF-2 interactions with the AR-NTD (AR N/C-terminal interactions) are essential for the transactivational properties of the receptor (12,13).

The major ligand-induced LBD conformational change required to attain a transcriptionally active receptor is the stabilization of the C-terminal helix, helix 12 (H12), in a precise position and orientation that completes the AF-2 surface (14–16). This helix exhibits significant mobility in the absence of ligand and is misplaced in an alternate conformation in response to antagonist binding (16–18). Thus, the dynamic properties of H12 determine the activation ability of nuclear receptors. H12 of the AR-LBD, however, has been observed only in the agonist conformation in all AR-LBD (agonist- or antagonist-bound) crystal structures solved to date (9 and references therein).

In this study, we describe the analysis of two substitutions, P892A and P892L, in the AR-LBD, identified in two unrelated individuals with CAIS. AR-P892 is N-terminally adjacent to H12 (N-capping H12) (Fig. 1B) where all substitutions reported so far are associated with a CAIS phenotype (19,20). We have used a combined approach including kinetic and biochemical analyses as well as molecular dynamic (MD) simulations to unravel the molecular basis of AR dysfunction in both mutants.

RESULTS

AR mutations

Two unrelated XY individuals with unambiguously female external genitalia were diagnosed with CAIS. Genital skin fibroblasts (GSFs) derived from each patient were examined for underlying AR abnormalities. Both GSF strains were cultured and assayed for androgen-binding properties using the synthetic androgens mibolerone (MB) and methyltrienolone (MT; R1881), as previously described (21). Both strains exhibited negligible androgen binding suggesting mutations in the AR-LBD coding sequences (exons 4–8). To identify these mutations, exons 4–8 of the *AR* from each GSF strain were polymerase chain reaction (PCR)-amplified and sequenced as previously described (21). Alternate single-point mutations were identified in an identical codon in exon 8 of the *AR* in each patient. These mutations resulted in the substitution of proline 892 (*CCG*) by alanine (*GCG*) in one patient (P892A) and by leucine (*CTG*) in the other (P892L). Each of the identified substitutions was incorporated separately into the pcDNA3-hAR mammalian expression vector. We have also reconstructed our previously reported mutant AR (K883X), which contains a premature stop codon resulting in a truncated-AR lacking H12 (AR-ΔH12) and was identified in a CAIS case (21). The AR-ΔH12, as expected, had no ligand-binding or transactivational activity and was included as a negative control.

The effects of AR-P892 substitutions on androgen binding

To evaluate the effect of AR-P892 substitutions on the mutant receptors' androgen-binding properties, we measured

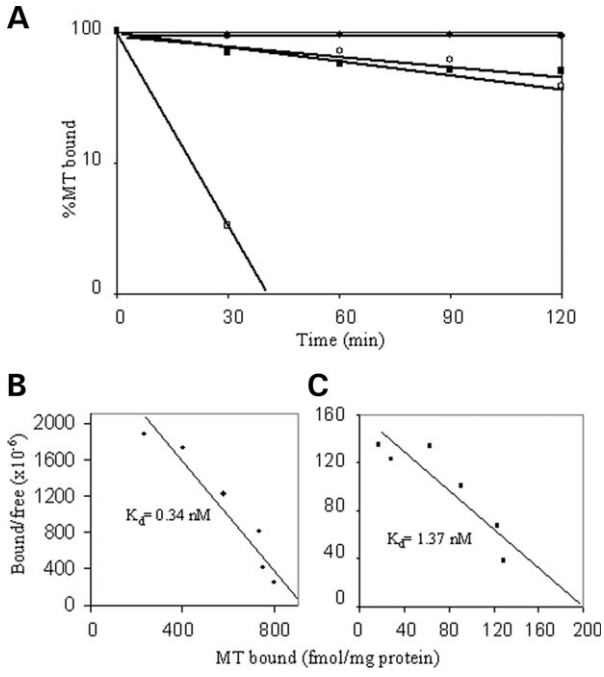

Figure 2. MT-binding properties of the wild-type and P892A mutant receptors in transfected COS-1 cells. (**A**) Rate constants of dissociation (k) at 37°C for wild-type (open circle) and P892A (open square) and at 22°C for wild-type (filled circle) and P892A (filled square). (**B** and **C**) Apparent equilibrium dissociation constants (K_d) for wild-type and P892A receptors, respectively. The AR-P892L mutant showed no binding at both temperatures.

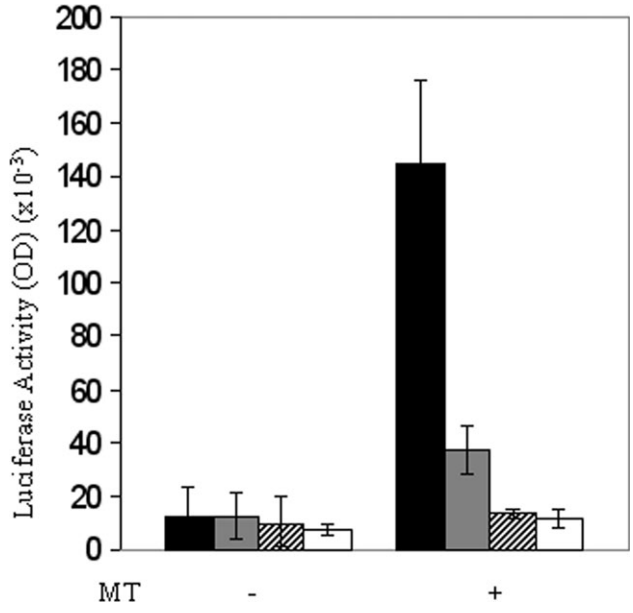

Figure 3. Transactivational properties of the wild-type and mutant ARs. The ability of the full-length wild-type and mutant ARs to transactivate an MMTV-Luciferase reporter gene in cotransfected COS-1 cells was assessed in the absence and presence of 3 nM MT. The mean ± SD of three different experiments for the wild-type (black), AR-P892A (gray), AR-P892L (striped) and AR-ΔH12 (white) in the presence and absence of 3 nM MT.

maximum androgen-binding capacity (B_{max}), rate constant of dissociation (k) and equilibrium dissociation constants (K_d) for the wild-type and mutant ARs in DNA-transfection studies. These studies revealed kinetic abnormalities for both mutant receptors. The P892A substitution resulted in a mutant receptor with low total binding and increased rate constant of dissociation and equilibrium dissociation constants [for methyltrienolone (MT) at 37°C in transfected COS-1 cells: $B_{max} < 20\%$ of wild-type; $k = 0.093 \pm 0.006$ versus 0.006 ± 0.0004 min^{-1} and $K_d = 1.37 \pm 0.03$ versus 0.34 ± 0.04 nM for P892A and wild-type ARs, respectively] (Fig. 2). Similar results were obtained in GSFs and when MB was used (data not shown). The effect of P892L substitution on the receptor's kinetics was more severe and resulted in a complete loss of androgen binding. In an attempt to slow the mutant receptors' dissociation rates for further analysis, we assessed their ligand-binding properties at lower temperatures. Although lower temperatures resulted in a partial enhancement in androgen-binding properties of the P892A receptor ($B_{max} > 40\%$ versus $<20\%$ of wild-type AR and $k = 0.008$ versus 0.093 at 22 and 37°C, respectively), P892L and AR-ΔH12 mutant receptors failed to bind ligand at both temperatures (Fig. 2A). The abnormalities of the mutant receptors were not due to expression or instability problems as revealed by western analysis (data not shown).

Transactivational activity of the mutant receptors

The ability of the mutant receptors to transactivate an MMTV-Luciferase reporter gene in cotransfected COS-1 cells in the presence of 3 nM MT was consistent with their kinetic profiles. AR-P892A substitution reduced luciferase activation by ∼80% compared with that of the wild-type AR (Fig. 3). The AR-P892L and AR-ΔH12 receptors were unable to activate transcription of the reporter gene.

MD simulation of the wild-type and mutant AR-LBDs

We investigated the structural and dynamic abnormalities associated with each substitution by performing MD simulations over 4 ns of the wild-type and the two mutant (P892A and P892L) AR-LBDs. The energies of the wild-type and two mutant proteins leveled off after about 2 ns, indicative of reaching an equilibrium state (data not shown). Visual inspection of the wild-type and mutant LBDs' structures showed that the global fold remained essentially intact. Inspection of time-dependent residue fluctuations (root mean-square deviations, RMSDs) from the average MD structures did not reveal marked differences between the three proteins. Also, MD-extracted B-factors, which provide a time-averaged representation of per-residue fluctuations, indicated less thermal motion relative to the crystal structure in all the three simulations. Focused examination of RMSD values for H12 (residues 892–908) of the wild-type and mutant LBDs over a period of 4 ns revealed a clear RMSD jump for both mutants that occurred between 1.5 and 2 ns (Fig. 4A). H12 of the AR-P892A exhibited larger RMSD fluctuations compared with that of the wild-type or AR-P892L mutant LBDs suggesting greater H12 mobility. In the AR-P892L, the RMSD jump was followed by a plateau starting at ∼2 ns, suggesting that H12 may be stabilized in a different

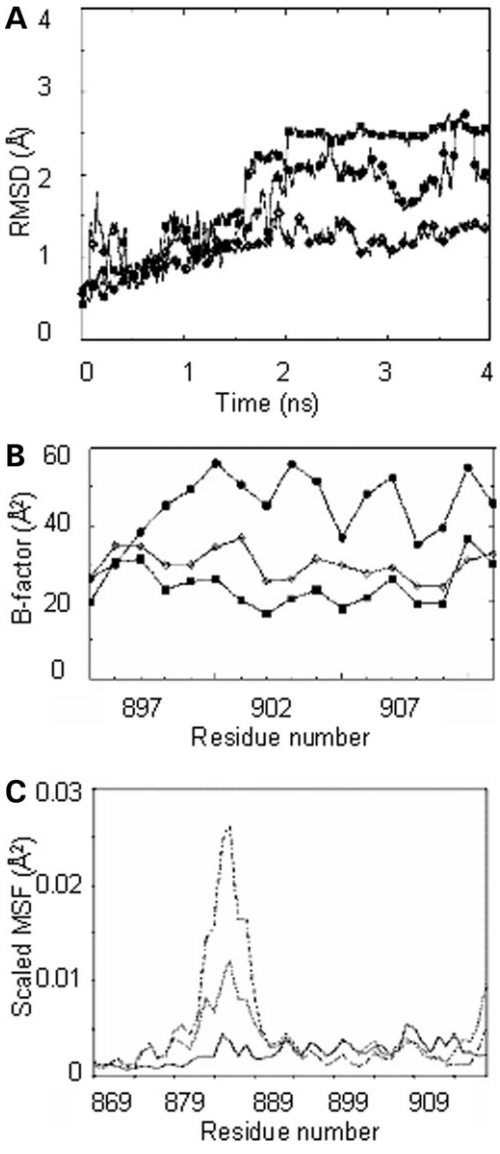

Figure 4. H12 deviation and flexibility for the wild-type and mutant LBDs. (**A** and **B**) RMSD values of the H12 C_α atoms during the 4 ns MD simulations and *B*-factors computed from the last 2 ns of MD simulations for the wild-type (open diamonds), AR-P892A (filled circles) and AR-P892L (filled squares). (**C**) Scaled C_α MSFs for residues 889–908 (including H11/H12 loop and H12) of the wild-type (solid line), AR-P892A (dotted line) and AR-P892L (dashed line) LBDs. The scaling of MSFs was done with respect to the sum of MSFs taken over all residues in the LBD.

(perturbed) conformation (Fig. 4A). Comparison of *B*-factors calculated over the last 2 ns of MD simulation revealed that although H12 of the AR-P892L mutant is more rigid than that of the wild-type, AR-P892A has a significantly more flexible H12 (Fig. 4B). More pronounced differences in the RMSDs were observed when H11–12 loops and the C-terminal extensions (residues 889–918) were included in the analysis (data not shown). Normal mode analysis revealed higher flexibility of H11–12 loop and H12 backbone for each mutant, which was more profound for the P892A substitution (Fig. 4C).

To examine H12 structural distortions and the integrity of AF-2 surfaces, structures averaged over the last nanosecond of MD simulations of the wild-type and mutant LBDs were visually inspected (22). P892L-H12 assumed a non-helical conformation (Fig. 5C), whereas P892A-H12 retained its helical structure but showed an overall backbone shift (Fig. 5B) compared with the wild-type H12 position (Fig. 5A). (φ, ψ) dihedral angle analysis of the trajectory revealed that the φ angles of residues I898 and I899 in H12 of the AR-P892L fluctuated about values of −140 and −110, respectively, which are non-helical dihedral angles (Supplementary Material, Fig. S1).

Analysis of helix 3 RMSDs in the three LBD models revealed no marked differences in helix 3 dynamics and flexibility (Supplementary Material, Fig. S2). Similar results were obtained for helix 4 (data not shown). However, a comparison of per-residue *B*-factors suggested slightly lower flexibilities for some AF-2 residues such as K720 (helix 3) and V730 (helix 4) in both mutant LBDs (Supplementary Material, Fig. S3). This may indicate a reduced capacity for the side-chain reorientations necessary for AR-NTD and/or coactivator binding in both mutants. To further assess AF-2 surfaces of the wild-type and mutant LBDs, the average distances between the main charge-clamp residues, K720 (helix 3) and E897 (helix 12), flanking the hydrophobic cleft of AF-2 were compared. Relative to the wild-type (21.29 Å) (Fig. 6A), the distance between centers of mass was increased (24.76 Å) for AR-P892A (Fig. 6B) and decreased (20.28 Å) for AR-P892L (Fig. 6C). Visual inspection also revealed that the hydrophobic AR-M894 strikingly disrupts the negative charge cluster of the AR-P892L mutant (by separating residues E893 and E709) (Fig. 6C). Although individual snapshots of side chains at the protein surface indicate significant flexibility, the average structures over the last nanosecond of MD simulations do show statistically significant differences between the wild-type and mutant structures. In order to account for solvation effects (especially important for surface side chains), the generalized Born (GB) continuum dielectric implicit solvation model was used (23).

We investigated the impact of each substitution on the H-bonding network of the ligand and around position 892 over the last 2 ns of the simulations. The MD simulation of the wild-type AR-LBD maintained the key H-bonds between the ligand-binding pocket and the ligand, T877 (helix 11) and N705 (helix 3) at the 17 β-hydroxyl group and R752 (helix 5) at its O3 group (6) (Fig. 7A). The mutant MD simulations revealed that the H-bond between AR-T877 and the ligand was destroyed by both substitutions (Fig. 7B and C). However, the lack of this H-bond may not explain the severe kinetic abnormalities we have observed for both mutant receptors. The absence of this H-bond in the well-characterized prostate cancer mutation, AR-T877A, results in no significant changes in the mutant receptor's binding affinities for testosterone, dihydrotestosterone (DHT) and MT (24). In addition to the loss of this H-bond, the AR-T877A substitution increases the space around the D-ring of the ligand, which may explain its promiscuous ligand-binding ability (7). Analysis around position 892 revealed that both substitutions created a hydrogen bond with N705 (helix 3). The new bond replaces the H-bond between N705 (helix 3) and D890 (H11–12 loop) in the wild-type receptor (Fig. 7).

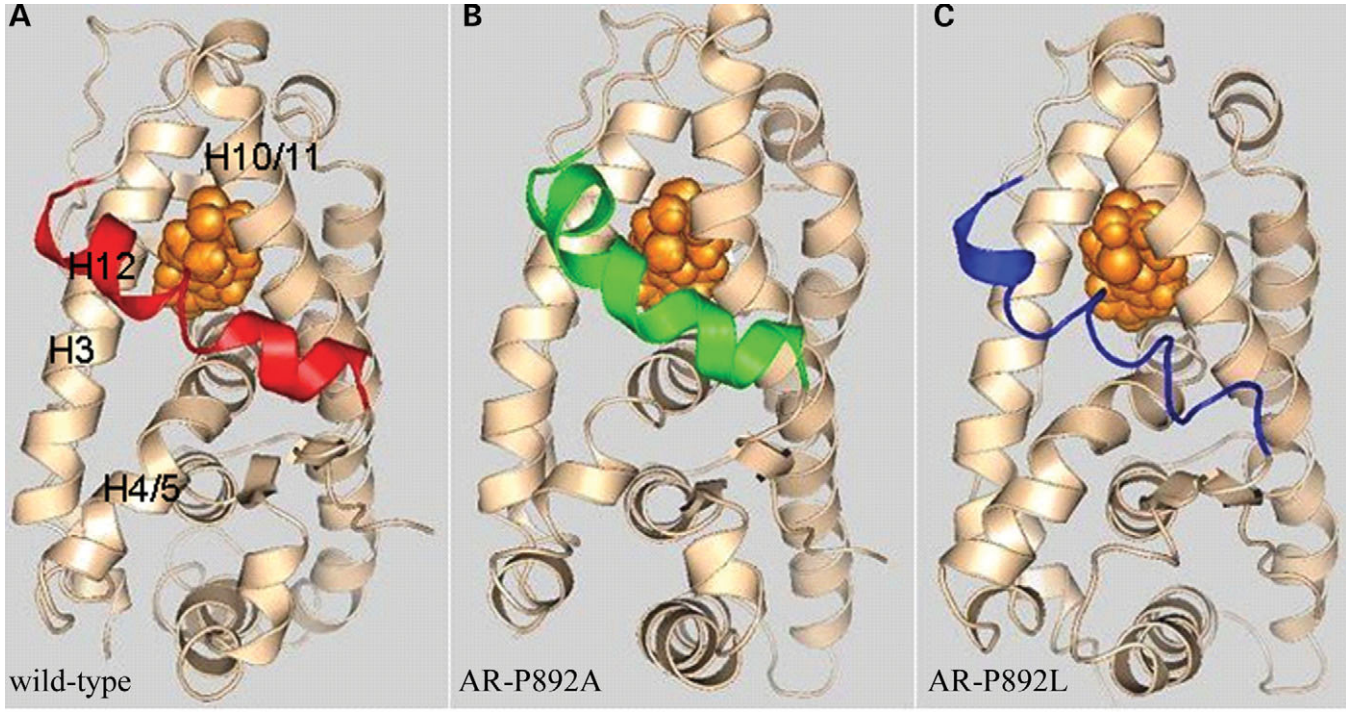

Figure 5. Average structures taken over the fourth nanosecond of the MD simulations for (**A**) the wild-type (H12 in red), (**B**) AR-P892A (H12 in green) and (**C**) AR-P892L (H12 in blue). The ligand (MT) is displayed in orange.

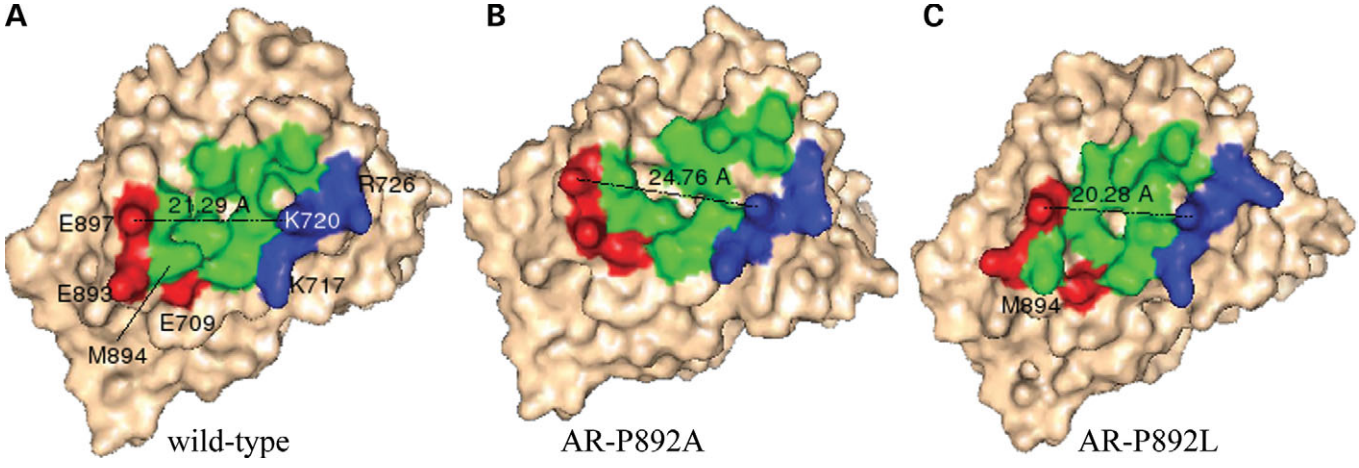

Figure 6. AF-2 surfaces of the wild-type and mutant AR-LBDs. The hydrophobic cleft (green), and flanking negative (red) and positive (blue) charge clusters are shown for the average structures over the fourth nanosecond of MD simulations for (**A**) wild-type, (**B**) AR-P892A and (**C**) AR-P892L LBDs. The average distances taken over the fourth nanosecond between centers of mass of residues K720 and E897 are shown. Average distances between E897 and M894 were 6.55, 7.07 and 7.27 Å for wild-type, AR-P892A and AR-P892L, respectively. Analogous trends (but higher fluctuations) were found when distances between charged groups were measured.

Calculation of averaged ligand-binding energies at room temperature revealed higher energies for AR-P892A and AR-P892L LBDs by 0.3 and 0.83 kcal/mol, respectively, compared with that of the wild-type LBD. Although by no means quantitatively accurate because the computed energy differences fall within the error range for this type of simulations, these results are in agreement with the decrease and lack of ligand binding at room temperature for AR-P892A and AR-P892L, respectively.

AR-H12 interactions with wild-type and mutant AR-DBD-LBD

The MD simulations suggest that the overall structures of the mutant liganded-LBDs remained intact with the exception of H12 misplacement. Thus, although helices 3, 4 and 5 of the AF2 domain appear to be in an accommodating position, the mutants' substitutions interfered with the proper ligand-induced placement of H12. H12 constraints are likely

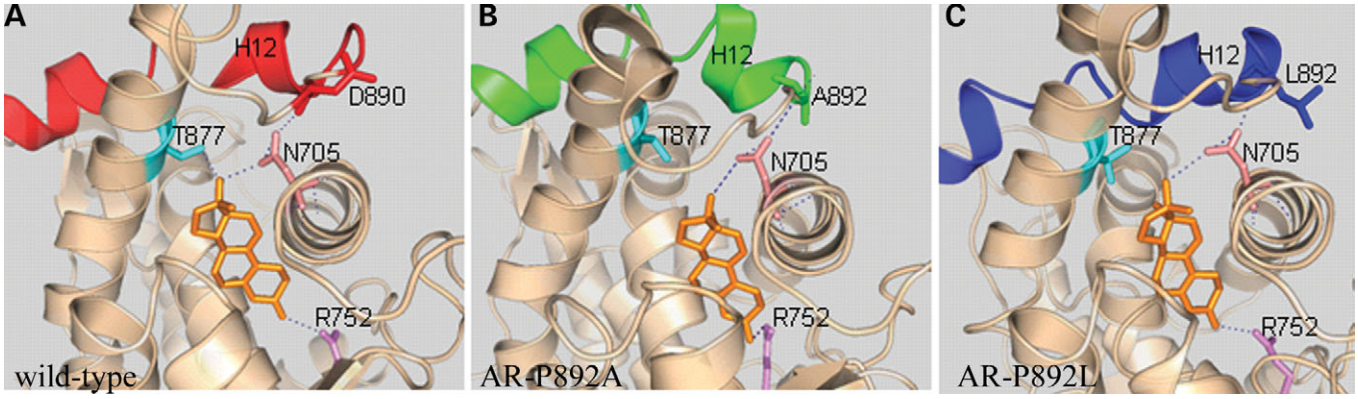

Figure 7. The hydrogen-bond network around residue 892 and within the ligand-binding pocket in (**A**) wild-type, (**B**) AR-P892A and (**C**) AR-P892L LBDs. Hydrogen bonds (dotted lines) were analyzed over the fourth nanosecond of MD simulations. The ligand is shown in orange and H12 is colored in red, green and blue for the wild-type, P892A and P892L, respectively. For clarity, hydrogen atoms are not displayed.

to be mediated by *cis*-acting elements within the LBD domain (see Discussion). Extrinsic (*in-trans*) wild-type H12 free of *cis* constraints should interact more competently with the H12-docking site on the mutant-LBD surface than the intrinsic (*in-cis*) mutant H12. The ability of an *in-trans* H12 to interact with an accommodating LBD surface has been previously observed in the glucocorticoid receptor LBD-dimer crystals where H12 swapping occurred between the identical subunits (18).

To assess the potential placement or misplacement of H12 that may be inherent to specific AR mutations, we employed the mammalian-two-hybrid system to develop a new *in vivo* assay that evaluates the accessibility of H12-docking site on the AR-LBD surface (Fig. 8). In the absence of ligand, both wild-type and AR-ΔH12 mutant LBDs were able to interact with an *in-trans* AR-H12 peptide (Fig. 9). Addition of ligand induces immediate repositioning of the wild-type *in-cis* H12 precluding the *in-trans* AR-H12 peptide interaction. In the AR-ΔH12, these interactions were preserved upon ligand addition as there is no *in-cis* H12 to be had. Similar to AR-ΔH12, both mutant LBDs were able to accommodate the *in-trans* AR-H12 peptide in the absence or presence of ligand (Fig. 9). This suggests that H12 is unable to reside in the active position in both mutants and thereby does not interfere with the binding of the *in-trans* AR-H12 in the presence of ligand. These results do indeed support our modeling studies predicting an improper structure for P892L-H12 and an increased mobility for P892A-H12.

DISCUSSION

This study describes the structural and functional properties of AR-P892A and AR-P892L mutant receptors and investigates the molecular basis for their association with CAIS phenotype. One of these substitutions, AR-P892A, is a novel mutation. Substitutions reported previously at this position (P892L and P892S) have also been associated with the complete form of AIS (19,20).

Kinetic and transactivational analyses of both mutant ARs revealed severe abnormalities that are consistent with the CAIS phenotype in each patient. The effect of P892L substitution on the receptor's kinetics was more severe resulting in complete loss of androgen binding even at lower temperature. The AR-P892A mutant receptor exhibited low total binding that was partially enhanced at lower temperatures.

These functional abnormalities are not surprising considering the conservation and location of the AR-P892 residue. It is conserved not only among the AR subfamily [progesterone receptor (PR), mineralocorticoid receptor (MR) and glucocorticoid receptor (GR)] but also in other nuclear receptors such as thyroid receptors (TRα and β), retinoic acid receptors (RARα, β and γ), retinoic acid-related orphan receptor 1 (ROR1) and liver X receptors (LXRα and β) (25,26).

The AR-P892 is located at a conserved critical position: the N-terminal cap of H12 (Fig. 1B). As revealed by structural and functional studies of the LBDs of the steroid receptors, H12 dynamic properties are the major determinant of the activation mode of these receptors (10,14–16). H12 exhibits high mobility and different conformations in the absence of ligand. Upon ligand binding, H12 is stabilized in a precise position to seal the ligand-binding pocket and finalize a hydrophobic surface that includes residues from helices 3, 4, 5 and 12 (15,27). Thus, a proline residue at the N-cap position of H12 may play a critical role in the integrity of the structure and flexibility of H12 required for its dynamic behavior. In fact, the AR-P892 (and the corresponding proline in GR and MR) is within a proline-box-motif (*hPxxhh*, where *P* is a proline at the N-cap position of the helix, *h* is a hydrophobic and *x* is any residue) that has been reported to contribute mainly to the orientation of the helix (28).

Furthermore, AR-P892 is in close proximity to three (F891, M895 and I899) out of 18 residues that are involved in LBD–ligand interactions (6). These residues and their ligand interactions are highly conserved in the GR, PR and MR (29–31). Thus, substitutions for AR-P892, and the corresponding proline in other receptors, may impair ligand binding by altering the interaction network between the receptor and its ligand.

The critical role for the AR-P892 is supported by the severe abnormalities associated with equivalent proline substitutions in other nuclear receptors (32,33). The MR-P957A results in a mutant receptor with impaired transcriptional activity even at

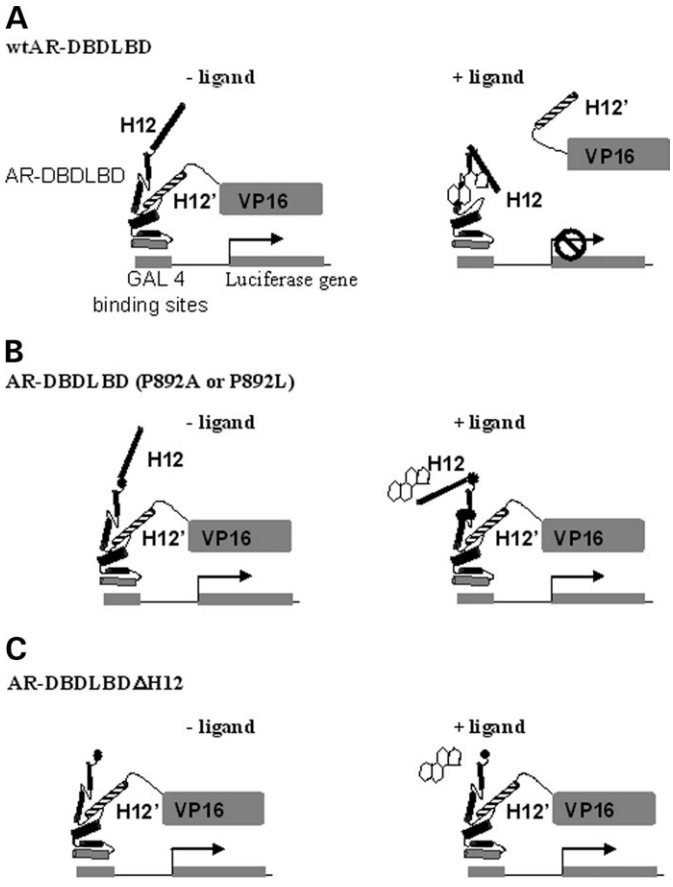

Figure 8. Novel *in vivo* interaction assay to assess the accessibility of H12-docking site on the AR-LBD surface. (**A**) The GAL4 DNA-binding domain (GAL4-DBD)-AR-DBD-LBD fusion protein binds to GAL4 DNA-binding sites. Interaction of the wild-type AR DBD-LBD with VP16-H12′ activates transcription of the luciferase reporter gene. Addition of ligand causes repositioning of the *in-cis* H12 (black), interfering with the *in-trans* H12′ (striped) interaction and prevent transcription of the reporter gene. (**B**) Misplacement of H12 in P892A and P892L mutants, and (**C**) lack of H12 in the AR DBD-LBDΔH12 prevent proper placement of the *in-cis* H12 allowing the *in-trans* H12′ to interact with the AR-DBD-LBD in the absence or presence of ligand.

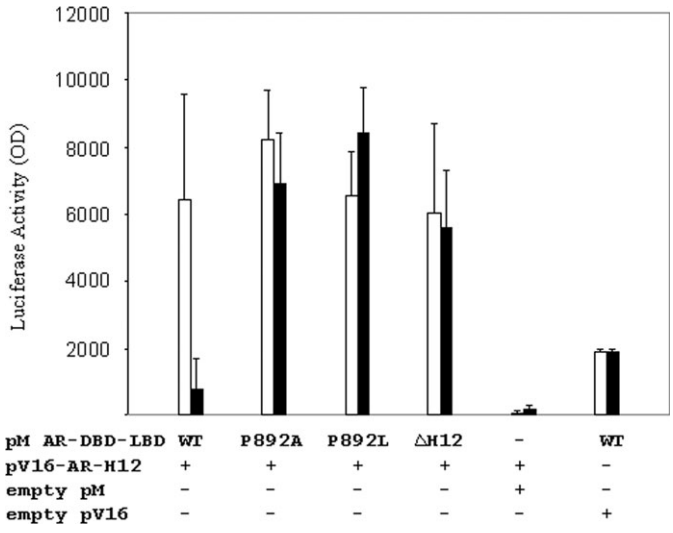

Figure 9. AR DBD-LBD:AR-H12 interactions for the wild-type and mutant AR DBD-LBD. Wild-type and mutant AR DBD-LBD interactions with an extrinsic AR-H12 peptide were assayed in cotransfected COS-1 cells in the absence and presence of ligand. The mean ± SD of three different experiments in the absence (white) and presence (black) of 10 nM MT.

high (1 μM) ligand concentration (33). TRβ-P457 mutants function as dominant negatives for the wild-type allele resulting in thyroid hormone resistance syndrome (34,35). Proline at the N-cap position may also be critical in H12 stabilization in constitutively active nuclear receptors. This has been shown for the RARβ where H12 adopts a closed conformation, preventing repression in the absence of ligand (32). A change of RARβ-P409 (corresponding to AR-P892) to serine resulted in H12 destabilization and target gene repression (32). Furthermore, proline substitutions at the adjacent positions in both ERα and PPARγ have been shown to result in severe consequences in the receptor transactivational properties (P892 of the AR is not conserved in these receptors) (17,36,37). The ERα-L536P mutation (corresponding to AR-F891) resulted in a receptor with constitutive activity and increased sensitivity to agonists (36). In contrast, the PPARγ-P467L substitution (corresponding to AR-E893) resulted in instability of H12 in the presence of ligand leading to a dominant negative effect causing severe insulin resistance and type II diabetes mellitus (17,37). The fact that proline substitutions result in target gene repression in the RARβ and a dominant negative effect in the TRβ and PPARγ may reflect the ability of these receptors, unlike steroid receptors, to bind DNA in the absence of ligand (38). The dominant negative affect, however, does not occur naturally in the AR due to the fact that the *AR* is an X-linked gene. Thus there is one *AR* allele in males and only one *AR* copy is expressed in females due to random X-inactivation.

To investigate the critical, and probably common, structural and dynamic differences associated with substitutions for this proline, we carried out nanosecond-scale MD simulations of the wild-type and the two mutant (P892A and P892L) AR-LBDs complexed with MT. The binding abnormalities for the AR-P892A and AR-P892L may result from alterations within their ligand-binding pockets, altered interactions with the ligand and/or structural abnormalities in the entry/exit gateways of the ligand. We simulated the ligand-bound form of AR-P892L mutant irrespective of our binding data, because even at weak affinities (e.g. millimolar K_d) the predominant form is still the ligand-bound one and hence is the proper form to use in the computer simulations. This is not inconsistent with the functional point of view where such low levels of affinity essentially exhibit the effects of complete loss of binding. We also note that the crystal structure of un-liganded AR-LBD is unavailable thus far.

Comparison of the three MD models revealed remarkable differences that are consistent with the kinetic and functional analyses of these mutants. The AR-P892L substitution resulted in more severe abnormalities where H12 assumed non-helical structure and was stabilized in a perturbed position (Fig. 5). The non-helical structure of P892L′-H12′ may explain the fact that this mutant behaved similar to the

AR-ΔH12 mutant in its complete lack of binding to both MT and MB at different temperatures. The stabilization of P892L-H12 in a perturbed position may result from misplaced interactions mediated by H12 itself or by its C-terminal extension (CTE). Normally, the AR-CTE stabilizes H12 in the active conformation by interacting with H8–9 loop, a mechanism that is conserved in the AR subfamily (6,29,39,40). The perturbed position for P892L-H12 may be stabilized in an inactive position by similar CTE-mediated interactions with the same or a different docking site. A recent report has shown that the repressive function of RARα in the absence of ligand is due to H12 stabilization in an open conformation by its CTE-mediated interactions (41). In contrast, the increased mobility exhibited by P892A-H12 may explain the fast dissociation rates and decreased transactivational properties for AR-P892A mutation. Despite its increased flexibility, P892A-H12 does retain a helical structure, albeit somewhat displaced, consistent with the partial androgen-binding capability.

The AF-2 surface of the AR includes a conserved hydrophobic cleft flanked by opposing-charge clusters: E897 and E893 (helix 12) and E709 (helix 3) on one side, K720 and K717 (helix 3) and R726 (helix 3–4 loop) on the other (8,11). The precise settings of these residues are critical for coactivator-binding and AR-N/C terminal interactions (8,11). The altered distances between the main charge-clamp residues, K720 (helix 3) and E897 (helix 12), and reduced flexibilities exhibited by some AF-2 residues in both mutant LBDs are likely to impair AF-2 interactions with coactivators and/or AR-NTD.

Analysis of the H-bond network around residue 892 revealed that a critical bond between N705 (H3) and D890 (H11–12 loop) was replaced in both mutant LBDs by an H-bond between the mutant residue and N705. The N705-D890 H-bond is important in the stabilization of the H11–12 loop of the AR (6). The AR-N705 is conserved in all members of the AR subfamily and appears to play similar roles in H11–12 loop stabilization in these receptors (Fig. 1B). The corresponding N719 of the PR is involved in an equivalent bond with PR-E904 (corresponding to AR-D890) that stabilizes H11–12 loop of the PR (6). Similar to PR, GR and MR have a glutamic acid corresponding to AR-D890. Thus, the absence of N705-D890 H-bond is likely to result in an increased H11–12 loop mobility leading to H12 instability in both mutant liganded-LBDs. This is supported by the increased flexibility of the loop revealed by the normal mode analysis. Stabilization of H11–12 loop rather than H12 has been suggested to be required for the NR-LBDs to assume and maintain an active conformation (39). The ligand-induced conformational changes of the NR-LBD appear to be mediated by *cis* elements within the LBD that act as 'microdevices' (42). One of these devices is positioned within the H11–12 loop which controls the flexibility of the downstream H12 (42). In contrast, the alternative H-bond created by either substitution may prevent a precise rotation and/or shifting of the 892 residue that is required for an accurate H12-repositioning. The H-bond replacement may also change the orientation of N705, which is still H-bonded to the ligand in both mutants. This may result in altered orientation of the ligand and may explain the loss of the H-bond between the ligand and T877 in both mutant LBDs. The AR-T877, which corresponds to a cysteine in the PR, MR and GR, is involved in ligand recognition and specificity (6).

The precise location and placement of H12 is central for the assembly and activation of the AF2 domain. H12 of unliganded (*apo*) steroid receptors is kept in an open conformation constricted from occupying a transactivationally active position required to complete the AF-2 surface. Addition of ligand relieves these constraints allowing for the proper placement of H12 and leading to AF2 domain activation. This is orchestrated by several molecular events dominated by the extensive movement of H12. The ligand-induced molecular events and the dramatic movement of H12 most likely require all essential elements to be *in-cis* with each other. Mutations suspected of deferring critical proper placement of the intrinsic *in-cis* H12, given that other molecular requirements are in place, may allow the mutant LBDs to accommodate an extrinsic *in-trans* H12. If indeed this is the case, one could infer that a specific mutation's inherent defect lies in the proper movement of its H12. Both AR-P892A and AR-P892L mutant receptors exhibited this property as shown by results of our H12 interaction assay.

Our combined kinetics and biochemical, as well as, MD simulation analyses show a clear correlation between the structural and functional abnormalities for both P892A and P892L mutant ARs and provide an explanation for the CAIS phenotype in both patients. Our data suggest that a proline residue as the N-cap of H12 may be critical not only in the AR but also in other nuclear receptors where this proline is conserved. To our knowledge, this is the first comprehensive structural and functional study for substitutions at this critical position. Combining classical kinetics and biochemical techniques with MD simulation models that are validated by *in vivo* studies, such as our H12 interaction assay, may provide a useful tool that is applicable and valuable to other members of the nuclear receptor family. The H12 interaction assay can be used to assess the inability of any mutant AR to inherently move H12 to its proper position.

MATERIALS AND METHODS

Identification of AR mutations

GSFs were cultured and maintained in Opti-MEM (GibcoBRL, Grand Island, NY). DNA was extracted and subjected to PCR amplification and direct sequencing of exons 4–8 of the *AR*, as previously described (21).

Mutant AR expression constructs

Each of the identified mutations (P892A and P892L) and our previously reported mutation (K883X; AR-ΔH12) (21) were incorporated separately into the full-length AR cDNA in pcDNA3-hAR expression vector, using the appropriate primers and the overlap extension method as described (43). The integration of the appropriate mutations was screened for using restriction enzymes; *BspM*II, abolished by P892 mutations, and *Mae*I, created by K883X mutation. The pcDNA3.1-AR-H12 vector was constructed to encode the

last 36 amino acids (aa 884–919) of the AR. This was done by PCR amplification using a primer designed to incorporate an *Eco*RI restriction site upstream of the desired AR sequence (884RI: 5′-GGAATTCACACATGGTGAGCGTGGAC-3′) and a primer located downstream of the AR sequence in the pSVhAR.BHEX vector (44) (P3′: 5′-CACCAACCTTCTGAT AGGCAGC-3′). The PCR product was double digested with *Eco*RI/*Sal*I and inserted into *Eco*RI/*Xho*I-digested pcDNA3.1 vector. Direct sequencing using the Thermo Sequenase Radiolabeled Terminator Cycle sequencing kit (USB Corp., Cleveland, OH, USA) was used to confirm the incorporation of only the desired sequences for all constructs.

Androgen-binding assays and cell transfections

Androgen-binding properties for both mutant receptors were assayed in cultured GSFs from each patient and in transfected COS-1 cells using the synthetic androgens MB and MT, as previously described (21). Binding assays in transfected COS-1 cells were performed at 37°C and room temperature, as previously described (43). Briefly, COS-1 cells were maintained in Opti-MEM (GibcoBRL) and plated, 24 h prior to transfection, in 6 and 12-well plates. Cells were transfected using Lipofectamine 2000 (GibcoBRL) as recommended by the manufacturer. All transfections included pCMV-β-galactosidase as a control for transfection efficiency. The stability of the mutant ARs was verified by western blotting of total proteins extracted from transfected COS-1 cells after incubation with and without 10 nM MT at 37°C in the presence of 100 μM cycloheximide for 24 and 48 h (43).

Transactivation assays

The transactivational properties of the mutant and wild-type ARs were evaluated in COS-1 cells cotransfected with an MMTV-Luciferase reporter vector. Cells were plated at a density of 3×10^5 cells/well in 12-well plates in Opti-MEM supplemented with 5% fetal bovine serum. The following day, cells were cotransfected with 300 ng wild-type or mutant full-length AR, 1 μg of pMMTV-Luc and 300 ng pCMV-β-galactosidase complexed with 4 μl LF2000 reagent per well. Twenty-four hours after transfection, the media was replaced by fresh media with and without 3 nM MT. Seventy-two hours after transfection, cells were harvested, lysed in 1× Reporter Lysis Buffer (Promega, Madison, WI, USA) and assayed for luciferase and β-gal activity according to Promega protocols (Promega). Total protein content was determined using BCA Protein Assay Kit (Pierce, Rockford, IL, USA).

MD simulations

The MD simulations for the wild-type, AR-P892A and AR-P892L LBDs were performed using AMBER 7.0 as previously described (45). The crystal structure of the AR-LBD complexed with MT was obtained from the Protein Data Bank (PDB entry: 1E3G) (6) and the disulfide bond between C669 and C844 removed as no evidence for its existence has been found in other AR-LBD structures (7,8). The AR-P892 substitutions were generated using SYBYL (SYBYL® 7.0, Tripos, Inc., Missouri, USA). The ligand was assigned general AMBER force field (GAFF) parameters and AM1/BCC charges using the Antechamber module in AMBER (23). Following bad-contact energy minimization, heating and equilibration, a 4 ns production run at 300 K was performed for each system. Snapshots of the systems were saved every 1 ps, and energy was recorded every 0.1 ps. The MD trajectories were processed using the PTRAJ module (for RMSDs, average structures, distances and dihedral angles) and the CARNAL module (for hydrogen bonds) from the AMBER package. MD-extracted *B*-factors were computed as

$$B_i = \left(\frac{8\pi}{3}\right)\langle (r_i(t) - \langle r_i \rangle)^2 \rangle$$

where i is the residue number and the angled brackets indicate time-averaged quantities. Structure visualization was performed using visual molecular dynamics (22) and Pymol (46). The analysis of ligand-binding energies was performed with the molecular mechanics Poisson–Boltzmann surface area (MM/PBSA) module from AMBER (23). One thousand MD snapshots (every 4 ps) for each system were extracted for the MM/PBSA calculations. The GB parameters used were a salt concentration of 0.2 M, an external dielectric of 80, a surface tension of 0.0072 and an off-set of 0. Non-polar contributions were calculated with the linear combinations of pairwise overlaps (LCPO) method in Sander. Ligand-binding energies were calculated as averages (over all MD snapshots) of the quantity $E_{\text{complex}} - (E_{\text{LBD}} + E_{\text{lig}})$, where 'complex' refers to the liganded-LBD.

Normal mode analysis

The normal mode analysis was performed using starting structures identical to those used for the MD simulations. The complexes were first energy-minimized using the AMBER95 potential, then optimized using a Beale restarted conjugate gradient algorithm. The potential function parameters were chosen to match the default parameters used during the MD simulations. All atoms were allowed to move during the minimizations, and no atomic constraints were applied. The convergence criterion was an all-atom grams of 1×10^{-4}. For each minimized complex, the $3N \times 3N$ analytical mass-weighted Hessian matrix of partial second derivatives was calculated, where N is the number of atoms in the complex (4155 for the wild-type complex, 4151 for P892A and 4160 for P892L). The eigenvectors corresponding to the three lowest frequencies of the non-trivial modes were used to calculate the mean-squared fluctuations (MSFs) for the Cα atom of each residue.

AR-DBD-LBD and AR-H12 two-hybrid constructs

The wild-type, P892A, P892L and AR-ΔH12 pM-AR-DBD-LBD vectors were constructed to code for the wild-type or mutant AR-DBD-LBD (aa 503–919) fused downstream and in-frame with the GAL4 DNA-binding domain (aa 1–147) in the pM vector (BD Biosciences Clontech, CA, USA). The mutations were introduced by *Bst*BI/*Xba*I double digestions of the corresponding mutant pcDNA3-hAR constructs and

religating in-frame with the similarly digested wild-type pM-AR-DBD-LBD. The pVP16-AR-H12 plasmid was constructed to code for aa 884–919 of the AR-fused in-frame with the coding sequence of the VP16 activation domain (aa 411–456) in pVP16 vector (BD Biosciences Clontech). This was done by extracting the AR fragment from the pcDNA3.1-AR-H12 vector by *Nco*I digestion and filling-in followed by *Pst*I digestion. The extracted fragment was then inserted into pVP16 vector that was digested with *Eco*RI and blunt-ended before digestion with *Pst*I.

AR-DBD-LBD:AR-H12 interaction assay

Interactions of AR-H12 with the AR-DBD-LBDs were tested *in vivo* using the mammalian two-hybrid system. This was done by cotransfecting the pM-AR-DBD-LBD (which contains the intrinsic *in-cis* H12) and the pVP16-AR-H12 (which contains the extrinsic *in-trans* H12). The pM-AR-DBD-LBDΔH12 (encoding AR aa 503–883) which lacks H12 in entirety was used as a control. COS-1 cells were plated in 6-well plates at a density of 5×10^5 cells/well. Transfections were performed, as described above, using 6 μl LF2000 reagent, 0.5 μg of wild-type or mutant pM-AR-DBD-LBD construct, 2 μg pVP16-AR-H12, 2 μg pGAL4-Luc reporter vector and 0.5 μg of pCMV-βgal per well. Empty pVP16 or pM vectors were used as controls. Twenty-four hours after transfection, fresh media, with and without 10 nM MT, was added to the transfected cells for 48 h. Luciferase and β-gal activity were assayed as described above.

SUPPLEMENTARY MATERIAL

Supplementary Material is available at HMG Online.

ACKNOWLEDGEMENTS

We thank Dr Lenore K. Beitel for helpful suggestions. Y.A.E. acknowledges full scholarship by the Secretariat of Education and Scientific Research of Libya (SESR). This work was supported by the Canadian Institutes for Health Research.

Conflict of Interest statement. None declared.

REFERENCES

1. Nuclear Receptors Nomenclature Committee (1999) A unified nomenclature system for the nuclear receptor superfamily. *Cell*, **16**, 161–163.
2. Quigley, C.A., De Bellis, A., Marschke, K.B., el-Awady, M.K., Wilson, E.M. and French, F.S. (1995) Androgen receptor defects: historical, clinical, and molecular perspectives. *Endocrinol. Rev.*, **16**, 271–321.
3. Gottlieb, B., Beitel, L.K., Wu, J.H. and Trifiro, M. (2004) The androgen receptor gene mutations database (ARDB): 2004 update. *Hum. Mutat.*, **23**, 527–533.
4. Boehmer, A.L., Brinkmann, O., Bruggenwirth, H., van Assendelft, C., Otten, B.J., Verleun-Mooijman, M.C., Niermeijer, M.F., Brunner, H.G., Rouwe, C.W., Waelkens, J.J. *et al*. (2001) Genotype versus phenotype in families with androgen insensitivity syndrome. *J. Clin. Endocrinol. Metab.*, **86**, 4151–4160.
5. Gottlieb, B., Beitel, L.K. and Trifiro, M.A. (2001) Variable expressivity and mutation databases: the androgen receptor gene mutations database. *Hum. Mutat.*, **17**, 382–388.
6. Matias, P.M., Donner, P., Coelho, R., Thomaz, M., Peixoto, C., Macedo, S., Otto, N., Joschko, S., Scholz, P., Wegg, A. *et al*. (2000) Structural evidence for ligand specificity in the binding domain of the human androgen receptor: implications for pathogenic gene mutations. *J. Biol. Chem.*, **275**, 26164–26171.
7. Sack, J.S., Kish, K.F., Wang, C., Attar, R.M., Kiefer, S.E., An, Y., Wu, G.Y., Scheffler, J.E., Salvati, M.E., Krystek, S.R. Jr *et al*. (2001) Crystallographic structures of the ligand-binding domains of the androgen receptor and its T877A mutant complexed with the natural agonist dihydrotestosterone. *Proc. Natl Acad. Sci. USA*, **98**, 4904–4909.
8. He, B., Gampe, R.T., Jr, Kole, A.J., Hnat, A.T., Stanley, T.B., An, G., Stewart, E.L., Kalman, R.I., Minges, J.T. and Wilson, E.M. (2004) Structural basis for androgen receptor interdomain and coactivator interactions suggests a transition in nuclear receptor activation function dominance. *Mol. Cell.*, **16**, 425–438.
9. Bohl, C.E., Gao, W., Miller, D.D., Bell, C.E. and Dalton, J.T. (2005) Structural basis for antagonism and resistance of bicalutamide in prostate cancer. *Proc. Natl Acad. Sci. USA*, **102**, 6201–6206.
10. Gronemeyer, H., Gustafsson, J.A. and Laudet, V. (2004) Principles for modulation of the nuclear receptor superfamily. *Nat. Rev. Drug. Discov.*, **3**, 950–964 (Review).
11. Estebanez-Perpina, E., Moore, J.M., Mar, E., Delgado-Rodrigues, E., Nguyen, P., Baxter, J.D., Buehrer, B.M., Webb, P., Fletterick, R.J. and Guy, R.K. (2005) The molecular mechanisms of coactivator utilization in ligand-dependent transactivation by the androgen receptor. *J. Biol. Chem.*, **280**, 8060–8068.
12. Ghali, S.A., Gottlieb, B., Lumbroso, R., Beitel, L.K., Elhaji, Y., Wu, J., Pinsky, L. and Trifiro, M.A. (2003) The use of androgen receptor amino/carboxyl-terminal interaction assays to investigate androgen receptor gene mutations in subjects with varying degrees of androgen insensitivity. *J. Clin. Endocrinol. Metab.*, **88**, 2185–2193.
13. Berrevoets, C.A., Doesburg, P., Steketee, K., Trapman, J. and Brinkmann, A.O. (1998) Functional interactions of the AF-2 activation domain core region of the human androgen receptor with the amino-terminal domain and with the transcriptional coactivator TIF2 (transcriptional intermediary factor 2). *Mol. Endocrinol.*, **12**, 1172–1183.
14. Warnmark, A., Treuter, E., Wright, A.P. and Gustafsson, J.A. (2003) Activation functions 1 and 2 of nuclear receptors: molecular strategies for transcriptional activation. *Mol. Endocrinol.*, **17**, 1901–1909.
15. Egea, P.F., Klaholz, B.P. and Moras, D. (2000) Ligand–protein interactions in nuclear receptors of hormones. *FEBS Lett.*, **476**, 62–67.
16. Brzozowski, A.M., Pike, A.C., Dauter, Z., Hubbard, R.E., Bonn, T., Engstrom, O., Ohman, L., Greene, G.L., Gustafsson, J.A. and Carlquist, M. (1997) Molecular basis of agonism and antagonism in the oestrogen receptor. *Nature*, **389**, 753–758.
17. Kallenberger, B.C., Love, J.D., Chatterjee, K.K. and Schwabe, J.W.R. (2003) A dynamic mechanism of nuclear receptor activation and its perturbation in a human disease. *Nat. Struct. Biol.*, **10**, 136–140.
18. Kauppi, B., Jakob, C., Farnegardh, M., Yang, J., Ahola, H., Alarcon, M., Calles, K., Engstrom, O., Harlan, J., Muchmore, S. *et al*. (2003) The three-dimensional structures of antagonistic and agonistic forms of the glucocorticoid receptor ligand-binding domain: RU-486 induces a transconformation that leads to active antagonism. *J. Biol. Chem.*, **278** (25), 22748–22754.
19. Peters, I., Weidemann, W., Romalo, G., Knorr, D., Schweikert, H.U. and Spindler, K.D. (1999) An androgen receptor mutation in the direct vicinity of the proposed C-terminal alpha-helix of the ligand binding domain containing the AF-2 transcriptional activating function core is associated with complete androgen insensitivity. *Mol. Cell. Endocrinol.*, **148**, 47–53.
20. Kanayama, H., Naroda, T., Inoue, Y., Kurokawa, Y. and Kagawa, S. (1999) A case of complete testicular feminization: laparoscopic orchiectomy and analysis of androgen receptor gene mutation. *Int. J. Urol.*, **6**, 327–330.
21. Trifiro, M., Prior, R.L., Sabbaghian, N., Pinsky, L., Kaufman, M., Nylen, E.G., Belsham, D.D., Greenberg, C.R. and Wrogemann, K. (1991) Amber mutation creates a diagnostic *Mae*I site in the androgen receptor gene of a family with complete androgen insensitivity. *Am. J. Med. Genet.*, **40**, 493–499.
22. Humphrey, W., Dalke, A. and Schulten, K. (1996) VMD—visual molecular dynamics. *J. Mol. Graph.*, **14**, 33–38.

23. Case, D.A., Pearlman, D.A., Caldwell, J.W., Cheatham, T.E., III, Wang, J., Ross, W.S., Simmerling, C.L., Darden, T.A., Merz, K.M., Stanton, R.V. *et al*. (2002) *AMBER7 User Manual*. University of California, San Francisco.
24. He, B., Gampe, R.T., Jr, Hnat, A.T., Faggart, J.L., Minges, J.T., French, F.S. and Wilson, E.M. (2005) Probing the functional link between androgen receptor coactivator and ligand binding sites in prostate cancer and androgen insensitivity. *J. Biol. Chem*., epub ahead of print, PMID 16365032, in press
25. Wurtz, J.M., Bourguet, W., Renaud, J.P., Vivat, V., Chambon, P., Moras, D. and Gronemeyer, H. (1996) A canonical structure for the ligand-binding domain of nuclear receptors. *Nat. Struct. Biol.*, **3**, 206.
26. Mi, L.Z., Devarakonda, S., Harp, J.M., Han, Q., Pellicciari, R., Willson, T.M., Khorasanizadeh, S. and Rastinejad, F. (2003) Structural basis for bile acid binding and activation of the nuclear receptor FXR. *Mol. Cell.*, **11**, 1093–1100.
27. Nolte, R.T., Wisely, G.B., Westin, S., Cobb, J.E., Lambert, M.H., Kurokawa, R., Rosenfeld, M.G., Willson, T.M., Glass, C.K. and Milburn, M.V. (1998) Ligand binding and co-activator assembly of the peroxisome proliferator-activated receptor-gamma. *Nature*, **395**, 137–143.
28. Viguera, A.R. and Serrano, L. (1999) Stable proline box motif at the N-terminal end of alpha-helices. *Protein Sci.*, **8**, 1733–1742.
29. Bledsoe, R.K., Montana, V.G., Stanley, T.B., Delves, C.J., Apolito, C.J., McKee, D.D., Consler, T.G., Parks, D.J., Stewart, E.L., Willson, T.M. *et al*. (2002) Crystal structure of the glucocorticoid receptor ligand binding domain reveals a novel mode of receptor dimerization and coactivator recognition. *Cell*, **110**, 93–105.
30. Williams, S.P. and Sigler, P.B. (1998) Atomic structure of progesterone complexed with its receptor. *Nature*, **393**, 392–396.
31. Fagart, J., Huyet, J., Pinon, G.M., Rochel, M., Mayer, C. and Rafestin-Oblin, M.E. (2005) Crystal structure of a mutant mineralocorticoid receptor responsible for hypertension. *Nat. Struct. Mol. Biol.*, **12**, 554–555.
32. Farboud, B., Hauksdottir, H., Wu, Y. and Privalsky, M.L. (2003) Isotype-restricted corepressor recruitment: a constitutively closed H12 conformation in retinoic acid receptors beta and gamma interferes with corepressor recruitment and prevents transcriptional repression. *Mol. Cell. Biol.*, **23**, 2844–2858.
33. Hellal-Levy, C., Fagart, J., Souque, A., Wurtz, J.M., Moras, D. and Rafestin-Oblin, M.E. (2000) Crucial role of the H11–H12 loop in stabilizing the active conformation of the human mineralocorticoid receptor. *Mol. Endocrinol.*, **14**, 1210–1221.
34. Chatterjee, V.K. (1997) Resistance to thyroid hormone. *Horm. Res.*, **48** (Suppl. 4), 43–46 (Review).
35. Yoh, S.M. and Privalsky, M.L. (2002) Molecular analysis of human resistance to thyroid hormone syndrome. *Methods Mol. Biol.*, **202**, 129–152 (Review).
36. Eng, F.C., Lee, H.S., Ferrara, J., Willson, T.M. and White, J.H. (1997) Probing the structure and function of the estrogen receptor ligand binding domain by analysis of mutants with altered transactivation characteristics. *Mol. Cell. Biol.*, **17**, 4644–4653.
37. Barroso, I., Gurnell, M., Crowley, V.E., Agostini, M., Schwabe, J.W., Soos, M.A., Maslen, G.L., Williams, T.D., Lewis, H., Schafer, A.J. *et al*. (1999) Dominant negative mutations in human PPARgamma associated with severe insulin resistance, diabetes mellitus and hypertension. *Nature*, **402**, 880–883.
38. Baniahmad, A. (2005) Nuclear hormone receptor co-repressors. *J. Steroid. Biochem. Mol. Biol.*, **93**, 89–97 (Review).
39. Tahiri, B., Auzou, G., Nicolas, J.C., Sultan, C. and Lupo, B. (2001) Participation of critical residues from the extreme C-terminal end of the human androgen receptor in the ligand binding function. *Biochemistry*, **40**, 8431–8437.
40. Sartorato, P., Cluzeaud, F., Fagart, J., Viengchareun, S., Lombes, M. and Zennaro, M.C. (2004) New naturally occurring missense mutations of the human mineralocorticoid receptor disclose important residues involved in dynamic interactions with deoxyribonucleic acid, intracellular trafficking, and ligand binding. *Mol. Endocrinol.*, **18**, 2151–2165.
41. Farboud, B. and Privalsky, M.L. (2004) Retinoic acid receptor-alpha is stabilized in a repressive state by its C-terminal, isotype-specific F domain. *Mol. Endocrinol.*, **18**, 2839–2853.
42. Costantino, G., Entrena-Guadix, A., Macchiarulo, A., Gioiello, A. and Pellicciari, R. (2005) Molecular dynamics simulation of the ligand binding domain of farnesoid X receptor: insights into helix-12 stability and coactivator peptide stabilization in response to agonist binding. *J. Med. Chem.*, **48** (9), 3251–3259.
43. Elhaji, Y.A., Wu, J.H., Gottlieb, B., Beitel, L.K., Alvarado, C., Batist, G. and Trifiro, M.A. (2004) An examination of how different mutations at arginine 855 of the androgen receptor result in different androgen insensitivity phenotypes. *Mol. Endocrinol.*, **18**, 1876–1886.
44. Kazemi-Esfarjani, P., Trifiro, M.A. and Pinsky, L. (1995) Evidence for a repressive function of the long polyglutamine tract in the human androgen receptor: possible pathogenetic relevance for the (CAG)n-expanded neuronopathies. *Hum. Mol. Genet.*, **4**, 523–527.
45. Wu, J.H., Gottlieb, B., Batist, G., Sulea, T., Purisima, E.O., Beitel, L.K. and Trifiro, M. (2003) Bridging structural biology and genetics by computational methods: an investigation into how the R774C mutation in the AR gene can result in complete androgen insensitivity syndrome. *Hum. Mutat.*, **22**, 465–475.
46. DeLano, W.L. (2002) The PyMOL Molecular Graphics System. DeLano Scientific, San Carlos.